Acta Crystallographica Section F
Structural Biology and Crystallization Communications
ISSN 1744-3091

Crystallization and preliminary X-ray crystallographic analysis of hydroquinone dioxygenase from *Sphingomonas* sp. TTNP3

Stefano Da Vela,[a] Marta Ferraroni,[a]* Boris A. Kolvenbach,[b] Eva Keller,[b] Philippe F. X. Corvini,[b] Andrea Scozzafava[a] and Fabrizio Briganti[a]

[a]Dipartimento di Chimica 'Ugo Schiff', Università di Firenze, Via della Lastruccia 3, 50019 Sesto Fiorentino FI, Italy, and [b]Institute for Ecopreneurship, School of Life Sciences, University of Applied Sciences and Arts Northwestern Switzerland, Gründenstrasse 40, 4132 Muttenz, Switzerland

Correspondence e-mail: marta.ferraroni@unifi.it

Received 2 March 2012
Accepted 21 March 2012

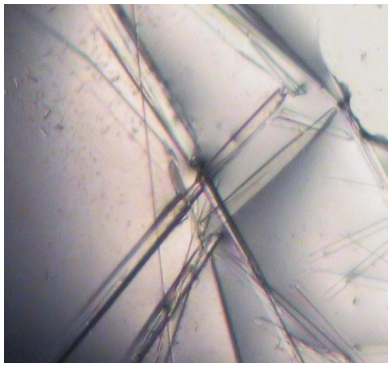

Hydroquinone dioxygenase (HQDO), a novel Fe^{II} ring-fission dioxygenase from *Sphingomonas* sp. strain TTNP3 which oxidizes a wide range of hydroquinones to the corresponding 4-hydroxymuconic semialdehydes, has been crystallized. The enzyme is an $\alpha_2\beta_2$ heterotetramer constituted of two subunits of 19 and 38 kDa. Diffraction-quality crystals of HQDO were obtained using the sitting-drop vapour-diffusion method at 277 K from a solution consisting of 16% PEG 4000, 0.3 *M* $MgCl_2$, 0.1 *M* Tris pH 8.5. The crystals belonged to the monoclinic space group $P2_1$, with unit-cell parameters a = 88.4, b = 125.4, c = 90.8 Å, β = 105.3°. The asymmetric unit contained two heterotetramers, *i.e.* four copies of each of the two different subunits related by noncrystallographic 222 symmetry. A complete data set extending to a maximum resolution of 2.5 Å was collected at 100 K using a wavelength of 0.980 Å.

1. Introduction

HQDO from *Sphingomonas* sp. TTNP3 catalyses the conversion of hydroquinone and of several alkylated and chlorinated hydroquinones to the corresponding 4-hydroxymuconic semialdehydes (see Fig. 1).

Since several pollutants of environmental concern are degraded *via* a hydroquinone pathway, HQDO is an enzyme of potential importance in the field of bioremediation. *Sphingomonas* sp. strain TTNP3 is able to degrade nonylphenol and bisphenol A, which are well known endocrine disruptors. In these degradation pathways hydroquinone is formed as the result of an *ipso*-hydroxylation and detachment of a carbocationic intermediate (Kolvenbach *et al.*, 2007). Hydroquinone is also a key intermediate in the degradation of significant environmental pollutants such as 4-nitrophenol (Spain & Gibson, 1991), γ-hexachlorocyclohexane (Miyauchi *et al.*, 1999), 4-hydroxyacetophenone (Moonen *et al.*, 2008) and 4-aminophenol (Takenaka *et al.*, 2003).

HQDOs in general can be separated into two different classes, both of which contain Fe^{2+} ions. Members of type I are monomeric and are phylogenetically related to the extradiol catechol dioxygenases (Machonkin *et al.*, 2010). Furthermore, HQDOs belonging to this class are generally capable of converting the polychlorinated hydroquinones formed during degradation of pentachlorophenol and γ-hexachlorocyclohexane (Machonkin & Doerner, 2011). Members of the type II HQDOs consist of two different subunits that form an $\alpha_2\beta_2$ heterotetramer.

As a member of the latter type, HQDO from *Sphingomonas* sp. TTNP3 is composed of two different subunits of 19 and 38 kDa and represents the first enzyme of this type to be isolated from a *Sphingomonas* strain. The metal content, the apparent size and the

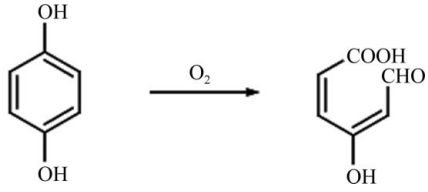

Figure 1
Ring-cleavage reaction catalysed by hydroquinone dioxygenase from *Sphingomonas* sp. strain TTNP3.

subunit composition suggest that the enzyme contains two active sites per heterotetramer. As in protocatechuate 4,5-dioxygenase and 2-amino-
phenol 1,6-dioxygenase, these active sites are likely to be positioned in the larger subunits, as has also been proposed for HQDO from *Pseudomonas fluorescens* strain ACB (Moonen *et al.*, 2008).

Type II HQDOs are novel members of a new family recently categorized as class III ring-cleaving dioxygenases (Ferraroni *et al.*, 2012). This family comprises gentisate dioxygenase, salicylate dioxygenase, 1-hydroxy-2-naphthoate dioxygenase, homogentisate dioxygenase, 3-hydroxyanthranilate dioxygenase, 4-amino-3-hydroxybenzoate 2,3-dioxygenase and flavonol 2,4-dioxygenase (Iwabuchi & Harayama, 1998; Hintner *et al.*, 2004; Fetzner, 2012). These enzymes are iron(II)-dependent enzymes and preferentially degrade *para*-diols or monohydroxylated aromatic carboxylic acids. Moreover, members of this family which have been structurally characterized are known to be part of the cupin superfamily, which is one of the most functionally diverse protein classes (Dunwell *et al.*, 2004) and features two highly conserved sequence motifs which form one functional metal-binding site (Adams *et al.*, 2006; Matera *et al.*, 2008; Li *et al.*, 2006; Titus *et al.*, 2000; Chen *et al.*, 2008; Ferraroni *et al.*, 2012). The cupin fold is composed of a motif of six to eight anti-parallel β-strands located within a conserved β-barrel structure.

HQDOs in general have not been thoroughly studied. Of the type II HQDOs, only those from *P. fluorescens* strain ACB and from *Sphingomonas* sp. strain TTNP3 have been purified and partially characterized to date (Moonen *et al.*, 2008; Kolvenbach *et al.*, 2011).

Here, we describe the crystallization and preliminary crystallographic analysis of a novel type II heterotetrameric HQDO isolated from *Sphingomonas* sp. strain TTNP3.

2. Materials and methods

2.1. Protein purification

HQDO from *Sphingomonas* sp. strain TTNP3 was purified, tested for activity and analysed for purity as described previously (Kolvenbach *et al.*, 2011). Briefly, cultures were grown on Standard I medium (Merck, Switzerland) and expression of HQDO was induced by the addition of 0.5 m*M* technical nonylphenol mixture (Fluka, Switzerland) 16 h prior to harvesting the cells at an OD_{550} of 2.5 (late exponential phase). Cell extract prepared from cells by sonication was brought to 40% ammonium sulfate saturation. After centrifugation, the supernatant was subjected to hydrophobic interaction chromatography on a Phenyl Sepharose HP column (GE Healthcare, Sweden); the enzyme activity eluted between 9 and 11% ammonium sulfate saturation. The active fractions were pooled and the activity eluted on a DEAE anion-exchange column (GE Healthcare, Sweden) between 250 and 300 m*M* NaCl. The active fractions were again pooled and the activity eluted on a MonoQ anion-exchange column (GE Healthcare, Sweden) between 400 and 450 m*M* NaCl. The apparently homogeneous enzyme was collected, desalted and concentrated by ultrafiltration (Amicon, 10 kDa cutoff; Millipore, USA).

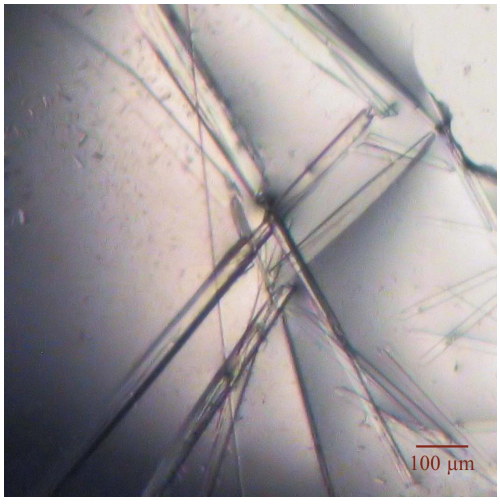

Figure 2
Crystals of hydroquinone dioxygenase from *Sphingomonas* sp. strain TTNP3 obtained using the sitting-drop vapour-diffusion method.

2.2. Crystallization

Crystallization experiments were performed using the sitting-drop vapour-diffusion method in 96-well plates (CrystalQuick, Greiner Bio-One, Germany). Drops were prepared using 1 µl protein solution mixed with 1 µl reservoir solution and were equilibrated against 100 µl precipitant solution. The protein concentration was 8 mg ml^{-1} in 25 m*M* Tris pH 7.0, 5 m*M* NaCl, 0.5 m*M* 4-hydroxybenzoic acid (an inhibitor preventing irreversible inactivation of the enzyme; Kolvenbach *et al.*, 2011; Moonen *et al.*, 2008). Initial crystallization trials were performed using the JCSG-plus Screen (Molecular Dimensions Ltd, UK) at 277 K. Diffraction-quality crystals were obtained from the following range of conditions: 12–20%(*w*/*v*) PEG 3350 or 14–16%(*w*/*v*) PEG 4000 or 6000 in the presence of 0.2–0.35 *M* $MgCl_2$ at different pH values ranging from 6.5 to 9.5 (the best choice was pH 9.0) using MES, HEPES, Tris and CHES (0.1 *M*) as the buffer.

2.3. Data collection

A complete data set was collected on the BM30 beamline, the ESRF, Grenoble using an ADSC Q315r CCD detector and a wavelength of 0.980 Å. For data collection, a crystal of the enzyme grown in a solution consisting of 14% PEG 6000, 0.3 *M* $MgCl_2$, 0.1 *M* Tris pH 8.5 was cooled to 100 K by inserting it into a nitrogen-gas stream; 20% glycerol was added to the mother-liquor solution as a cryoprotectant. The data were integrated and scaled using *XDS* (Kabsch, 2010).

3. Results and discussion

Needle-shaped crystals of HQDO from *Sphingomonas* sp. strain TTNP3 typically grew within 1 d at 277 K to approximate dimensions of 0.1 × 0.1 × 0.6 mm using the sitting-drop vapour-diffusion method (see Fig. 2). Frequently, prismatic crystals of a different habit were also present in the same drop, but were too small to be characterized.

The crystals belonged to the primitive monoclinic space group $P2_1$, with unit-cell parameters a = 88.4, b = 125.4, c = 90.8 Å, β = 105.3°. The asymmetric unit contained two heterotetramers (V_M = 2.13 $Å^3$ Da^{-1}, 42.3% solvent content; Matthews, 1968).

Data processing with *XDS* gave 67 837 unique reflections, an R_{merge} of 12.1% and an overall completeness of 97.9%. Statistics of data collection and processing are reported in Table 1.

The self-rotation function calculated with *MOLREP* (Vagin & Teplyakov, 2010) from the *CCP*4 program suite (Winn *et al.*, 2011) using a maximum resolution of 4.0 Å and an integration radius of 44.2 Å is shown in Fig. 3. The stereographic projections of the function only present sufficiently intense peaks in the section at κ = 180°, implying the presence of 222 noncrystallographic symmetry relating the four copies of each of the two different subunits in the

Table 1
Crystal parameters and data-collection statistics.

Values in parentheses are for the highest resolution shell.

Beamline	BM30, ESRF
Wavelength (Å)	0.980
Space group	$P2_1$
Unit-cell parameters (Å, °)	a = 88.4, b = 125.4, c = 90.8, β = 105.3
Asymmetric unit content	2 tetramers
V_M (Å^3 Da^{-1})	2.13
Solvent content (%)	42.3
Limiting resolution (Å)	50.00–2.46 (2.61–2.46)
Unique reflections	67837 (9734)
R_{merge}† (%)	12.1 (55.7)
R_{meas}‡ (%)	13.3 (61.4)
Completeness (%)	97.9 (87.6)
$\langle I/\sigma(I)\rangle$	13.33 (3.16)
Multiplicity	6.1 (5.5)

† $R_{merge} = \sum_{hkl}\sum_i |I_i(hkl) - \langle I(hkl)\rangle|/\sum_{hkl}\sum_i I_i(hkl)$, where $I_i(hkl)$ is an individual intensity measurement and $\langle I(hkl)\rangle$ is the average intensity for this reflection. ‡ $R_{meas} = \sum_{hkl}\{N(hkl)/[N(hkl)-1]\}^{1/2}\sum_i |I_i(hkl) - \langle I(hkl)\rangle|/\sum_{hkl}\sum_i I_i(hkl)$, where $I_i(hkl)$ is an individual intensity measurement, $\langle I(hkl)\rangle$ is the average intensity for this reflection and N is the multiplicity.

asymmetric unit. The two peaks along the y axis at (90, 90, 180°) and (90, 270, 180°) correspond to the crystallographic twofold screw axis. The remaining peaks can be interpreted as originating from the 222 noncrystallographic symmetry: two axes are responsible for the two peaks **p** (63.2, 90, 180°) and **q** (26.8, 270, 180°), whereas the third mutually perpendicular axis determines the two peaks labelled **r** that lie on the x axis corresponding to (90, 0, 180°) and (90, 180, 180°). The X peak on the c^* axis arises from the interaction of the crystallographic axis along b and the noncrystallographic axis along a. This axis generates the symmetry partners of the peaks **p** and **q** at coordinates **p**′ (63.2, 270, 180°) and **q**′ (26.8, 90, 180°).

The two subunits are not closely related to any other protein of known structure, so molecular-replacement techniques cannot be applied in order to solve the enzyme structure. For the larger subunit the highest similarity is to a domain of a murine T-cell receptor composed of 115 amino acids (PDB entry 1i9e), which shows an identity of 36.2% (Rudolph *et al.*, 2001). Sequence alignments also indicated significant identity of residues 258–323 of the large subunit to the sequence regions corresponding to the β-barrel cupin folds of

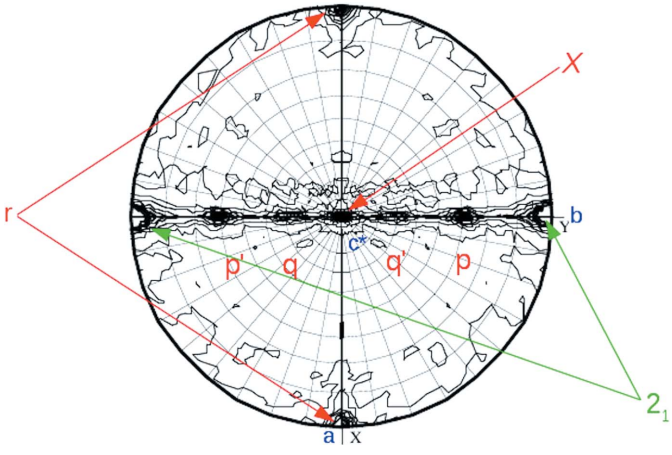

Figure 3
The κ = 180° section of the self-rotation function calculated with the program *MOLREP* using a 44.2 Å radius of integration and data in the resolution range 10.0–4.0 Å. The plot shows the peaks **p** (63.2, 90, 180°), **q** (26.8, 270, 180°) and **r** (90, 0, 180°) representing three mutually perpendicular axes. The X peak on the c^* axis arises from the interaction of the crystallographic axis along b (2_1) and the noncrystallographic axis along a (**r**). This axis generates the symmetry partners of the peaks **p** and **q** at coordinates **p**′ (63.2, 270, 180°) and **q**′ (26.8, 90, 180°).

3-hydroxyanthranilate and acidoreductone dioxygenase (23.9 and 26.8%, respectively). Hence, HQDO is likely to comprise a single cupin domain, *i.e.* it is a monocupin, in contrast to other ring-cleaving dioxygenases belonging to the cupin superfamily, such as salicylate, gentisate and 1-hydroxy-2-naphthoate dioxygenases, which are bicupins.

A complete data set was collected at a wavelength of 1.741 Å (the experimental iron absorption edge) on the BM30 beamline at the ESRF, Grenoble. A Patterson map calculated using this data set did not show any strong peak in the Harker section that could be attributed to the Fe^{2+} ions.

Currently, attempts are being made to find heavy-atom derivatives and to solve the structure using their anomalous signal in a MAD or SAD experiment depending on the accessibility of their absorption-edge wavelengths. Native PAGE experiments on the protein solution diluted with heavy-atom solutions as reported in Boggon & Shapiro (2000) are being applied in order to pre-screen the large number of possible different compounds.

We acknowledge the European Synchrotron Radiation Facility for the provision of synchrotron-radiation facilities and we would like to thank David Cobessi for assistance in using beamline BM30. Project co-funding by the European Commission within the 7th Framework Programme under Grant Agreement 265946 is acknowledged.

References

Adams, M. A., Singh, V. K., Keller, B. O. & Jia, Z. (2006). *Mol. Microbiol.* **61**, 1469–1484.
Boggon, T. J. & Shapiro, L. (2000). *Structure*, **8**, R143–R149.
Chen, J., Li, W., Wang, M., Zhu, G., Liu, D., Sun, F., Hao, N., Li, X., Rao, Z. & Zhang, X. C. (2008). *Protein Sci.* **17**, 1362–1373.
Dunwell, J. M., Purvis, A. & Khuri, S. (2004). *Phytochemistry*, **65**, 7–17.
Ferraroni, M., Matera, I., Steimer, L., Bürger, S., Scozzafava, A., Stolz, A. & Briganti, F. (2012). *J. Struct. Biol.* **177**, 431–438.
Fetzner, S. (2012). *Appl. Environ. Microbiol.* **78**, 2505–2514.
Hintner, J.-P., Reemtsma, T. & Stolz, A. (2004). *J. Biol. Chem.* **279**, 37250–37260.
Iwabuchi, T. & Harayama, S. (1998). *J. Biol. Chem.* **273**, 8332–8336.
Kabsch, W. (2010). *Acta Cryst.* D**66**, 125–132.
Kolvenbach, B. A., Lenz, M., Benndorf, D., Rapp, E., Fousek, J., Vlcek, C., Schäffer, A., Gabriel, F. L. P., Kohler, H. P. E. & Corvini, P. F. X. (2011). *AMB Express*, **1**, 8.
Kolvenbach, B., Schlaich, N., Raoui, Z., Prell, J., Zühlke, S., Schäffer, A., Guengerich, F. P. & Corvini, P. F. (2007). *Appl. Environ. Microbiol.* **73**, 4776–4784.
Li, X., Guo, M., Fan, J., Tang, W., Wang, D., Ge, H., Rong, H., Teng, M., Niu, L., Liu, Q. & Hao, Q. (2006). *Protein Sci.* **15**, 761–773.
Machonkin, T. E. & Doerner, A. E. (2011). *Biochemistry*, **50**, 8899–8913.
Machonkin, T. E., Holland, P. L., Smith, K. N., Liberman, J. S., Dinescu, A., Cundari, T. R. & Rocks, S. S. (2010). *J. Biol. Inorg. Chem.* **15**, 291–301.
Matera, I., Ferraroni, M., Bürger, S., Scozzafava, A., Stolz, A. & Briganti, F. (2008). *J. Mol. Biol.* **380**, 856–868.
Matthews, B. W. (1968). *J. Mol. Biol.* **33**, 491–497.
Miyauchi, K., Adachi, Y., Nagata, Y. & Takagi, M. (1999). *J. Bacteriol.* **181**, 6712–6719.
Moonen, M. J. H., Synowsky, S. A., van den Berg, W. A. M., Westphal, A. H., Heck, A. J. R., van den Heuvel, R. H. H., Fraaije, M. W. & van Berkel, W. J. H. (2008). *J. Bacteriol.* **190**, 5199–5209.
Rudolph, M. G., Huang, M., Teyton, L. & Wilson, I. A. (2001). *J. Mol. Biol.* **314**, 1–8.
Spain, J. C. & Gibson, D. T. (1991). *Appl. Environ. Microbiol.* **57**, 812–819.
Takenaka, S., Okugawa, S., Kadowaki, M., Murakami, S. & Aoki, K. (2003). *Appl. Environ. Microbiol.* **69**, 5410–5413.
Titus, G. P., Mueller, H. A., Burgner, J., Rodríguez De Córdoba, S., Peñalva, M. A. & Timm, D. E. (2000). *Nature Struct. Biol.* **7**, 542–546.
Vagin, A. & Teplyakov, A. (2010). *Acta Cryst.* D**66**, 22–25.
Winn, M. D. *et al.* (2011). *Acta Cryst.* D**67**, 235–242.